Improving Gene Delivery: Synergy between Alkyl Chain Length and Lipoic Acid for PDMAEMA Hydrophobic Copolymers

Prosper P. Mapfumo, Liên S. Reichel, Stephanie Hoeppener, and Anja Traeger*

In the field of gene delivery, hydrophobic cationic copolymers hold great promise. They exhibit improved performance by effectively protecting genetic material from serum interactions while facilitating interactions with cellular membranes. However, managing cytotoxicity remains a significant challenge, prompting an investigation into suitable hydrophobic components. A particularly encouraging approach involves integrating nutrient components, like lipoic acid, which is known for its antioxidant properties and diverse cellular benefits such as cellular metabolism and growth. In this study, a copolymer library comprising 2-(dimethylamino)ethyl methacrylate (DMAEMA) and lipoic acid methacrylate (LAMA), combined with either *n*-butyl methacrylate (*n*BMA), ethyl methacrylate (EMA), or methyl methacrylate (MMA), is synthesized. This enables to probe the impact of lipoic acid incorporation while simultaneously exploring the influence of pendant acyclic alkyl chain length. The inclusion of lipoic acid results in a notable boost in transfection efficiency while maintaining low cytotoxicity. Interestingly, higher levels of transfection efficiency are achieved in the presence of *n*BMA, EMA, or MMA. However, a positive correlation between pendant acyclic alkyl chain length and cytotoxicity is observed. Consequently, P(DMAEMA-*co*-LAMA-*co*-MMA), emerges as a promising candidate. This is attributed to the optimal combination of low cytotoxic MMA and transfection-boosting LAMA, highlighting the crucial synergy between LAMA and MMA.

P. P. Mapfumo, L. S. Reichel, S. Hoeppener, A. Traeger
Laboratory of Organic and Macromolecular Chemistry (IOMC)
Friedrich Schiller University Jena
Humboldtstrasse 10, 07743 Jena, Germany
E-mail: anja.traeger@uni-jena.de
S. Hoeppener, A. Traeger
Jena Center for Soft Matter (JCSM)
Friedrich Schiller University Jena
Philosophenweg 7, 07743 Jena, Germany

DOI: 10.1002/marc.202300649

1. Introduction

Gene therapy could revolutionize the treatment of acquired and inherited diseases, by introducing genetic material into specific cells to either correct malfunctioning or express deficient genes.[1–3] Delivery of the genetic material is mainly mediated by two classes of carriers, that are, viral and non-viral vectors. While both have their merits, non-viral vectors such as lipids, or cationic polymers, are a preferred choice due to their lower immunogenicity, ability to carry larger genetic payloads and inexpensive production.[4–7] Despite the lipids' remarkable performance to efficiently deliver mRNA or siRNA into cells, as demonstrated in the development of vaccines during the pandemic, their effectiveness in delivering plasmid DNA into cell nuclei is limited. This limitation has driven the relentless search for alternative transport vectors, with cationic polymers coming into focus as a promising solution.[8]

An ideal polymeric vector should complex and shield genetic material from serum interactions, facilitate cellular membrane internalization and endosomal escape, and release genetic material while remaining non-toxic.[9] To this end, cationic polymers such as poly(2-dimethylaminoethyl methacrylate) (PDMAEMA) have been broadly investigated due to their potential as a delivery vector.[10,11] While PDMAEMA demonstrates a notable binding affinity, its optimal performance as a carrier is attainable at higher molecular weights, leading to increased cytotoxicity due to membrane disruption.[12] Therefore, various strategies employing DMAEMA have been explored to enhance transfection efficiency while maintaining low cytotoxicity.[11] A promising approach for enhancing the transfection efficiency of cationic polymers involves incorporating hydrophobic components.[3,13] These cationic hydrophobic polymers form electrostatic interactions with genetic material and self-assemble, resulting in stable complexes that are resistant to serum interactions.[14–16] Furthermore, the hydrophobic components can interact with cellular membranes which leads to improved uptake or endosomal release.[16–19]

Among other hydrophobic groups, incorporating hydrophobic monomers with acyclic alkyl chains pendant groups such as
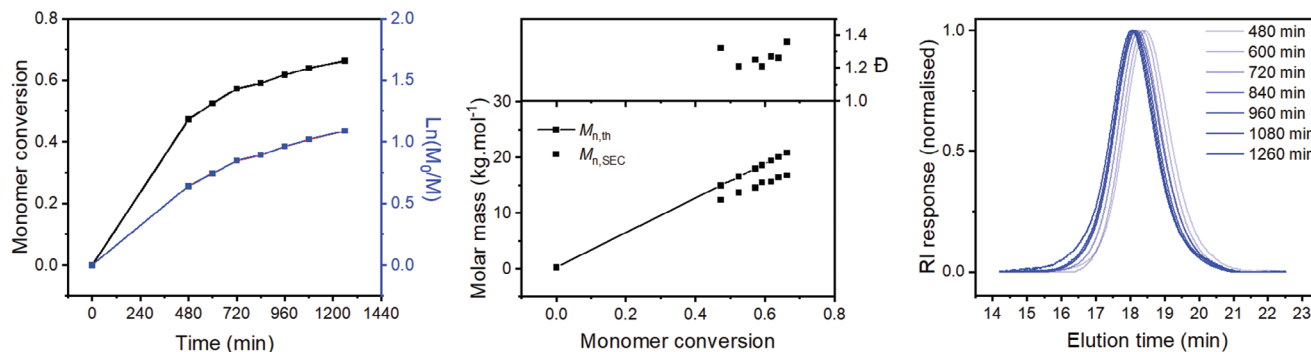
Figure 1. Summarized kinetics plot of P[(DMAEMA)$_x$-co-(nBMA)$_y$-co-(LAMA)$_z$]. The left plot depicts monomer conversion, the middle plot compares calculated and measured molar masses at various conversions, and the right plot displays SEC traces over time. Conversions were determined by ^{1}H NMR and molar mass distributions were measured by SEC using (DMAc + 0.21% LiCl) as eluent and PMMA calibration.

n-butyl methacrylate (nBMA) and methyl methacrylate (MMA) has proved beneficial in enhancing delivery performance. However, in some cases higher molar ratios of nBMA and/or MMA show increased toxicity.[16,17,20–22] To this end, integrating natural compounds such as lipoic acid as a hydrophobic group represents an interesting solution in maintaining low molar ratios of acyclic alkyl chains pendant groups. Further, it allows for the introduction of biological functions inherent to lipoic acid.[23–25] It is an endogenous antioxidant vital for mitochondrial energy metabolism, cell growth, and differentiation.[26,27] When integrated in a vector, lipoic acid's disulfide bond and ring structure facilitate its cellular uptake by interacting with exofacial thiols, augmenting its potential as a gene delivery agent.[28,29]

For example, Zheng and co-workers demonstrated that incorporating lipoic acid into polyethylenimine (PEI) enhances transfection efficiency with minimal cytotoxicity.[30] This aligns with findings from our previous study, which showcased an improved transfection efficiency and low cytotoxicity for a micelle consisting of DMAEMA, nBMA, and lipoic acid methacrylate (LAMA).[25]

In this study, we explore the incorporation of lipoic acid and acyclic alkyl groups into a hydrophobic cationic copolymer system to harness their potential for enhancing transfection. To maximize lipoic acid's potential, the design was modified to enhance cellular interaction, departing from our previous study where it was within a micelle's core. Furthermore, we examine how varying the length of pendant acyclic alkyl chains affects the properties of the polymer and its biological performance. We synthesized a copolymer library comprising DMAEMA and LAMA with either nBMA, EMA, or MMA as hydrophobic components. A subsequent biological investigation evaluated their interaction with genetic material, cytotoxicity, and transfection efficiency.

2. Results and Discussion

Reversible addition-fragmentation chain transfer (RAFT) polymerization technique was utilized for all syntheses owing to its versatility, ability to synthesize polymers with complex architectures, and narrow molar mass distributions.[31–33] First, a kinetic study was conducted with DMAEMA, LAMA, and nBMA as monomers to establish uniform reaction conditions for all polymerizations. The kinetics were performed over a 21 h period at

70 °C using 4-Cyano-4-[[(ethylthio)thioxomethyl]thio]pentanoic acid (CPAETC) as the chain transfer agent and 4,4′-azobis(4-cyanovaleric acid) (ACVA) as initiator (**Figure 1**).

The kinetics revealed similar reactivity among the monomers, irrespective of the pendant group type. Considering that all investigated monomers were methacrylates and exhibited comparable reactivity in terms of kinetics, the chosen conditions and substituents were deemed representative for subsequent polymerization reactions. However, the non-linearity of the semilogarithmic plot suggested a reduction in active propagating species over time due to termination reactions.[34] Consequently, the polymerization time was reduced to 15 h for subsequent reactions. Afterward, a small copolymer library, that is, P0-A, P0-B, and P1, composed of DMAEMA, LAMA, and nBMA was synthesized to conduct a preliminary transfection investigation (**Scheme 1** and Figure S1, Supporting Information). The composition builds upon our previous work, which involved a micelle delivery system.[25] Different molar ratios of DMAEMA (50%, 60%, and 70%) were employed, along with a corresponding equimolar ratio of nBMA and LAMA. In the initial screening of transfection, it was observed that transfection efficiency improved as the DMAEMA molar ratio increased and the molar ratios of nBMA and LAMA decreased. The order of transfection efficiency was as follows: P1 (52%) > P0-B (17%) > P0-A (5%) (Figure S2, Supporting Information). Consequently, the less efficient variants P0-A and P0-B (transfection efficiency <20%) were excluded from further studies and new polymers, P2–P7, were synthesized based on the promising composition of P1 (**Scheme 1**). The DMAEMA content was comparable for all polymers, while the hydrophobic side groups were varied.

In our previous work, the synergistic effect of copolymerizing nBMA and MMA with DMAEMA also proved advantageous in enhancing transfection.[22,35] Consequently, copolymers P1–P3 were designed and synthesized, incorporating nBMA, EMA, and MMA, respectively, to utilize their performance benefits, while simultaneously investigating the influence of pendant acyclic alkyl chain length on overall performance. On the other hand, polymers P4–P7 were devised as controls to investigate the specific impacts of LAMA (P4 and P5) and MMA (P6 and P7). Regarding polymerizations, monomer conversions were in the range of 65% to 70%. As summarized in **Table 1**, SEC traces (Figures S3–S6, Supporting Information) revealed good polymerization control,
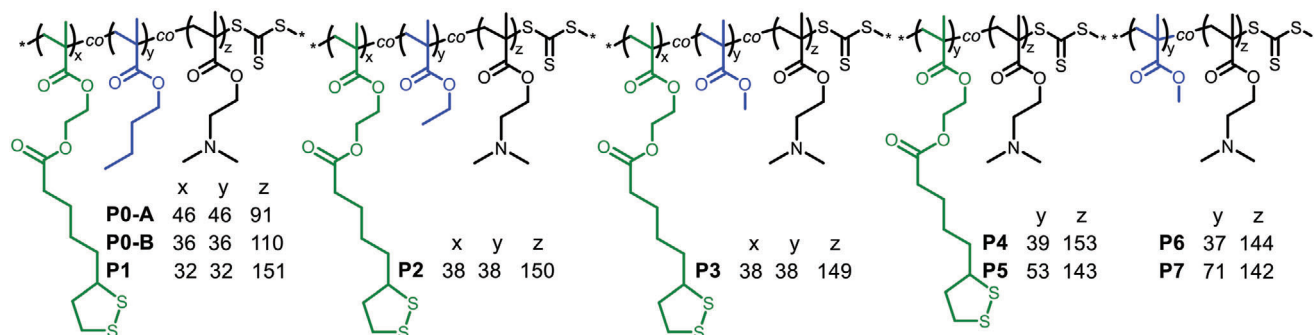
Scheme 1. The structures of the polymer library, (P0–P7) which was synthesized RAFT polymerization for 15 h at 70 °C using 4-cyano-4-[[(ethylthio)thioxomethyl]thio]pentanoic acid (CPAETC) as the chain transfer agent and 4,4′-azobis(4-cyanovaleric acid) (ACVA) as initiator.

with narrow molar mass distributions between 20–40 kg mol^{-1} and dispersities (Đ) below 1.4.

Since apparent pK$_a$ of nanoparticles show a high correlation with the efficacy and toxicity,[36,37] titration experiments were conducted to determine the apparent pK$_a$ values of all polymers (**Table 1** and Figure S7, Supporting Information). The hydrophobic nature of the polymers led to precipitation during the titrations, consequently reducing the ability of the DMAEMA moieties to be protonated/deprotonated, thus causing variations in the DoC values. The obtained values ranged from 7.0 to 7.4 for P1–P7, which is slightly below and comparable to the apparent pK$_a$ value of PDMAEMA, that is, 7.4.[11] Notably, the values are close to the optimal range for high performing lipids for gene delivery, that is, 6 to 7.[37] Nevertheless, both the apparent pK$_a$ values and the degree of charge (DoC) at pH 7.4 underscore the pH responsiveness of these polymers. This responsiveness is noteworthy since over 50% of DMAEMA units remain chargeable when the pH decreases, thus improving the buffering capacity. This is advantageous for pH-dependent endosomal release when considering the sponge-effect hypothesis mechanism.[38–41] On the other hand, a low DoC at physiological pH potentially leads to poor binding and consequently, potential loss of genetic material. This was evident for P0-A and P0-A, which showed inferior performance (Figure S2, Supporting Information). Despite binding being observed in the ethidium bromide assay (EBA), the heparin release assay (HRA) indicated a reduced stability compared

to the other polymers (further details in Table S1 and Figure S8, Supporting Information).

Prior to biological investigations of P1–P7, EBA was conducted to study the affinity of the polymer to the genetic material and HRA was performed to study the stability of the polymer-plasmid DNA (pDNA) complexes. A reduction in fluorescence intensity, which is associated with stronger binding, was observed starting at N*/P 3 (ratio of protonated amine in the polymer to phosphate in the pDNA) (Figure S9A, Supporting Information). As revealed by HRA, more heparin was required for complete pDNA release at higher N*/P ratios for P1–P7 (Figures S9B and S10, Supporting Information), showcasing stability of the polyplexes. Based on the aforementioned results and the preliminary transfection efficiency results of P1 (Figure S2, Supporting Information), it was concluded that an N*/P ratio of 5 was the optimal ratio for formulating fully complexed pDNA. As nanosized particles are preferred for higher biological impact, the polyplex sizes of P1–P7 complexes at an N*/P ratio of 5 were determined by dynamic light scattering (DLS). As shown in **Figure 2**, the results showed a Z-average hydrodynamic diameter within a range of 84–127 nm for P1–P7 with polydispersity indexes below 0.2 (further plots are shown in Figure S11, Supporting Information). The comparable sizes, particularly with P1–P6, are beneficial when investigating transfection efficiency, as they minimize the influence of nanoparticle size effect. Overall, the findings underscore the synergistic effect between electrostatic

Table 1. Summary of molar masses, pK$_a$ and degree of charge (DoC) values of the polymer library.

	$M_{n,th}$[a] [kg mol^{-1}]	$M_{n, SEC}$[b] [kg mol^{-1}]	Đ[c]	Apparent pK$_a$[d]	DoC[e] [%] (pH 7.4)
P0-A	35.6	17.9	1.3	6.4	—
P0-B	34.2	17.1	1.3	6.7	9
P1	39.0	34.1	1.3	7.2	26
P2	40.2	37.9	1.3	7.3	35
P3	39.4	37.3	1.3	7.0	12
P4	36.6	33.0	1.3	7.1	19
P5	40.2	39.5	1.4	7.3	38
P6	26.6	24.6	1.2	7.4	50
P7	29.7	20.9	1.3	7.4	49

[a] Calculated by Equation S1 (Supporting Information) using conversion determined by ^{1}H NMR; [b,c] Determined by SEC using DMAc (0.21 wt% LiCl) as eluent and PMMA standards for calibration; [d,e] Calculated by Equation S2 (Supporting Information) and determined by Figure S7 (Supporting Information).
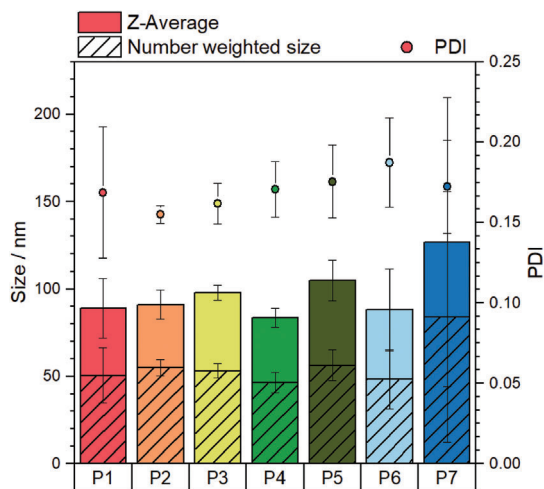
Figure 2. The DLS plot illustrates the Z-average with full-colored bars, number-weighted hydrodynamic diameters with patterned bars, and PDI with a dot plot ($n = 3$).
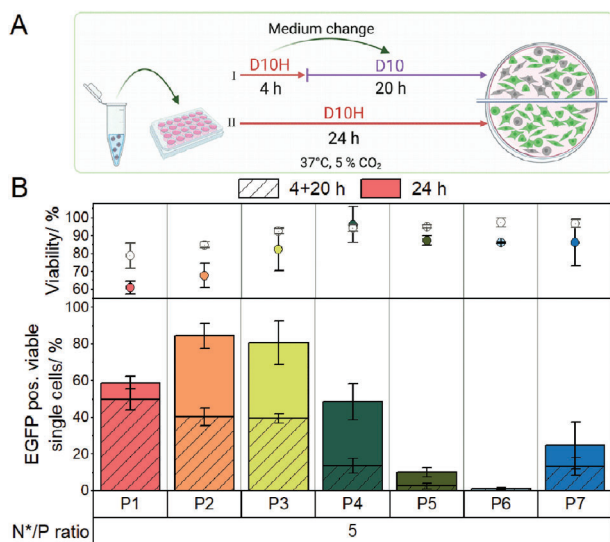

Figure 3. A) Experiment design of transfection efficiency assay: I) medium change after 4 h incubation (4 + 20 h) and II) 24 h transfection results in HEK293T cell line. B) Transfection efficiency (below) and viability conducted with CytoTox-ONE assay (above) of P1–P7 ($n \geq 3$). Further details are shown in Figures S12 and S13 (Supporting Information).

interactions and hydrophobic-induced self-assembly of polymers when binding genetic material, leading to the formation of small-sized nanoparticles.[3] Furthermore, the formulated polyplexes were within the optimal size range for efficient endosomal uptake.[42]

Transfection efficiencies of P1–P7 were assessed using a human embryonic kidney cell line HEK293T in Dulbecco's modified Eagle's medium supplemented with 10% serum (D10) and 10 mM 4-(2-hydroxyethyl)−1-piperazineethanesulfonic acid (D10H) to stabilize the pH value of the media. Polyplexes were incubated for 4 + 20 h (medium change to D10 after 4 h followed by further 20 h incubation) and 24 h (no medium change) as illustrated in **Figure 3A**. The transfection efficiencies were

assessed using pDNA encoding enhanced green fluorescent protein (mEGFP-N1 pDNA). Successful delivery of mEGFP-N1 pDNA to the nucleus leads to the expression of green fluorescent protein, which is quantified by flow cytometry. As such, improved transfection efficiency is an indicator of particle uptake, endosomal escape, and subsequent cargo release.[43] Before harvesting cells for flow cytometry analysis, aliquots were taken from the supernatant to conduct the CytoTox-ONE assay, a fluorometric-based method used to assess membrane integrity and, consequently, viability.

Figure 3B shows that after 4 + 20 h incubation, P1 exhibited a transfection efficiency marginally higher than P2 and P3, which showed similar transfection efficiencies. Interestingly, the associated cytotoxicity after 4 + 20 h incubation reveals that a decrease in pendant acyclic alkyl chain length, that is, replacing *n*BMA (P1) with EMA (P2) or MMA (P3) results in remarkable cytotoxicity alleviation. A similar trend among the three polymers was also observed after 24 h incubation. Expectedly, the longer incubation period resulted in increased cytotoxicity, with P1 and P2 demonstrating increased cytotoxicity compared to P3. On the other hand, with extended incubation (24 h), transfection efficiency of P2 and P3 increased by approximately by a factor of 2, while P1 showed only a slight increase. It was assumed that the efficacy of P1 was potentially obscured due to higher cytotoxicity. The observations imply that shorter pendant acyclic alkyl chain lengths enhance biocompatibility, thereby augmenting overall effectiveness. Furthermore, it is evident that an augmentation in acyclic alkyl chain length leads to increased cytotoxicity via membrane destabilization. This corroborates the research of Wakefield et al., who observed that an increase in alkyl chain length resulted in enhanced lytic membrane activity while studying amphiphilic polyvinyl ethers.[19] However, it is noteworthy that this active membrane attribute also contributes to improved transfection performance. Therefore, P3, with a shorter acyclic alkyl chain length (MMA) combined with LAMA, emerged as the most promising candidate, demonstrating an optimal membrane interaction, resulting in high transfection efficiency and relatively low cytotoxicity. As such, the morphology of P3 polyplexes was investigated by cryogenic transmission electron microscopy (cryo-TEM) and showed spherical polyplex particles (Figure S14, Supporting Information). Additionally, the spherical nanoparticles had an average size of 40 ± 13 nm, comparable to the number-weighted hydrodynamic diameter determined by DLS (53 ± 4 nm). The latter is considered more suitable for comparison with Cryo-TEM–determined hydrodynamic diameter because it reduces the effects of size-weighting factors. Furthermore, it should be noted that the nanoparticle hydration shell results in increased sizes in DLS measurements in comparison to cryo-TEM.[44,45]

When comparing the promising tri-copolymer, P3, to the control polymers, P4–P7, it is apparent that a combination of both MMA and LAMA exhibits synergistic effects for achieving enhanced performance with reduced cytotoxicity. Reduced cytotoxicity and transfection efficiency profiles were observed when only using LAMA or MMA for both short and long incubation times. Regarding their transfection efficiencies, increasing LAMA content, that is, P4 versus P5, unexpectedly results in a reduced transfection efficiency. Interestingly, a similar effect of reduced performance with increase in lipoic acid was observed by Zheng and
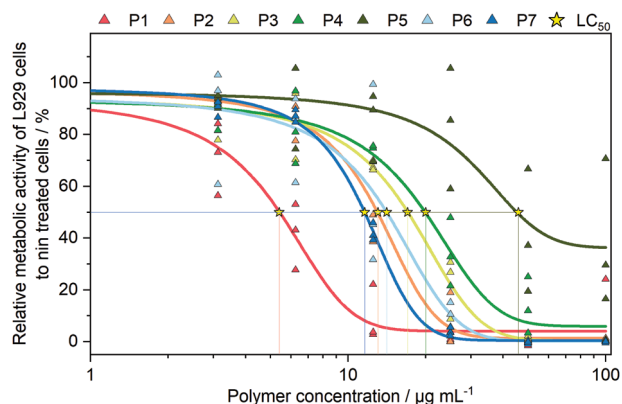
ADVANCED
SCIENCE NEWS

www.advancedsciencenews.com

Macromolecular
Rapid Communications

www.mrc-journal.de

Figure 4. PrestoBlue assay over 24 h in L929 cells. Dots represent values of single repetitions (*n* = 3), and lines represent Dose Respond fit function. Further details are shown in Figure S15 (Supporting Information). Stars indicate 50% cytotoxic polymer concentration (LC$_{50}$). LC$_{50}$ of PrestoBlue can be found on Table S2 (Supporting Information).

Figure 5. Pearson correlation matrix of P1 to P7. Analysis was done using OriginPro Software (Version 2022b). Orange circles show a direct correlation and blue circle show an inverse correlation. The bigger the circle and the more intense the color, the higher the direct/inverse correlation. Non-correlations were represented as dots. *apparent pK$_a$, **transfection efficiency of 24 h, ***differences between transfection efficiency of 4 + 20 h and 24 h.

colleagues, investigating the effect of coupled lipoic acid to PEI on transfection efficiency.[30] Contrastingly, when comparing polymers consisting of DMAEMA and MMA, it could be observed that increasing MMA, that is, P6 versus P7, results in increased transfection efficiency. Moreover, upon comparing the MMA copolymers, P6 and P7, with best-performing LAMA copolymer, P4, it is evident that incorporating LAMA into PDMAEMA notably improves both transfection efficiency and cell viability. Furthermore, it highlights the advantageous impact of integrating lipoic acid in enhancing performance, a phenomenon which was also noted in our previous research.[25]

Further assessment of cytotoxicity profiles of P1–P7 was achieved by CytoTox-ONE and PrestoBlue assays in a mouse fibroblast cell line L929 following ISO10993-5.[46] PrestoBlue assesses the relative metabolic activity of the cells, and the biochemical principle of the dye is similar to the CytoTox-ONE assay. However, in the latter case, the fluorescence intensity is observed in membrane damaged cells,[47] whereas in the PrestoBlue assay, metabolically inhibited cells affect the fluorescence intensity values, which reveals the PrestoBlue to be a more sensitive assay. As shown in **Figure 4**, generally, increase in polymer concentration resulted in a notable reduction in cell metabolic activity and disruption in membrane integrity. CytoTox-ONE assay also exhibited similar trends (Figure S15, Supporting Information). For comparability, it is worth noting that the polymer concentration range used during transfection investigations was between 10 and 12 µg mL^{-1}. Notably, the concentration utilized for the polymers remained below its LC$_{50}$, except for P1 (Table S2, Supporting Information). Overall, the presence of *n*BMA, EMA or MMA enhanced cytotoxicity in the order: *n*BMA>>EMA>MMA. In contrast, P5, with higher LAMA content, proved to be the least toxic polymer. This indicates that LAMA possesses low membrane disruptive properties and does not hinder cell metabolism to a similar extent as acyclic alkyl chains.

However, when comparing transfection efficiency and cytotoxicity results of P4–P7, a transfection efficiency-cytotoxicity dilemma can be observed since increase in LAMA improves viability but decreases transfection efficiency, while increasing MMA results in the opposite. This dilemma was circumvented
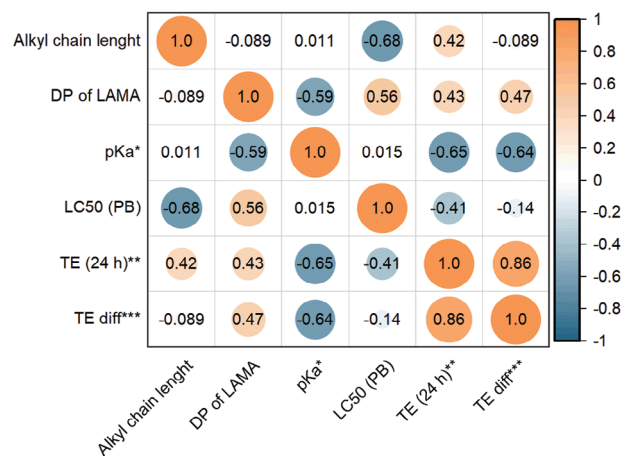
when both hydrophobic moieties were utilized to yield P3, P(DMAEMA$_{149}$-*co*-LAMA$_{38}$-*co*-MMA$_{38}$).

Our findings, presented in **Figure 5** as a Pearson correlation matrix, indicate distinct relationships. Comparing polymers P1–P3, an increase in pendant acyclic alkyl chain length led to enhanced transfection efficiency. However, this enhancement was accompanied by increased cytotoxicity, as evidenced by a stronger inverse correlation with LC$_{50}$ compared to a direct correlation with transfection efficiency (denoted as TE). Notably, varying chain length exerted minimal impact at shorter incubation periods, as denoted by the correlation with the differences between transfection efficiency of 4 +20 h and 24 h (denoted as TE diff) of P1-P3 . Furthermore, an inverse correlation emerged between the DP of LAMA and the apparent pK$_a$ due to the augmented hydrophobicity of LAMA, resulting in a reduction of pK$_a$. Remarkably, suitable apparent pK$_a$ values proved advantageous by improving cell internalization through hydrophobic interaction and facilitating endosomal escape. These factors directly correlated with both transfection efficiency and TE diff. Moreover, the incorporation of lipoic acid boosted transfection efficiency and increased viability.

3. Conclusion

In conclusion, polymer P3, P(DMAEMA$_{149}$-*co*-LAMA$_{38}$-*co*-MMA$_{38}$), showcased optimal performance, characterized by high transfection efficiency and low cytotoxicity. In contrast, P1 and P2 exhibited higher cytotoxicity, while P4–P7 demonstrated lower transfection efficiency but improved cytotoxicity. This highlighted the synergistic interplay between LAMA and MMA as pivotal for enhancing cationic polymers' efficacy in gene delivery. Our forthcoming investigations will concentrate on fine-tuning the polymer composition using LAMA as a hydrophobic modifier. Additionally, we will explore the potential advantages of lipoic acid through its polymer release for cellular metabolism, growth, and differentiation.[48]

4. Experimental Section

Materials, methods, and all experimental procedures are described in the Supporting Information.

Supporting Information

Supporting Information is available from the Wiley Online Library or from the author.

Conflict of Interest

The authors declare no conflict of interest.

Data Availability Statement

The data that support the findings of this study are available on request from the corresponding author. The data are not publicly available due to privacy or ethical restrictions.

[1] F. Arabi, V. Mansouri, N. Ahmadbeigi, *Biomed. Pharmacother.* **2022**, *153*, 113324.

[2] B. B. Mendes, J. Conniot, A. Avital, D. Yao, X. Jiang, X. Zhou, N. Sharf-Pauker, Y. Xiao, O. Adir, H. Liang, J. Shi, A. Schroeder, J. Conde, *Nat. Rev. Methods Primers* **2022**, *2*, 24.

[3] Z. Liu, Z. Zhang, C. Zhou, Y. Jiao, *Prog. Polym. Sci.* **2010**, *35*, 1144.

[4] H. Zu, D. Gao, *AAPS J.* **2021**, *23*, 78.

[5] H. Yin, R. L. Kanasty, A. A. Eltoukhy, A. J. Vegas, J. R. Dorkin, D. G. Anderson, *Nat. Rev. Genet.* **2014**, *15*, 541.

[6] D. W. Pack, A. S. Hoffman, S. Pun, P. S. Stayton, *Nat. Rev. Drug Discovery* **2005**, *4*, 581.

[7] M. A. Mintzer, E. E. Simanek, *Chem. Rev.* **2009**, *109*, 259.

[8] X. Hou, T. Zaks, R. Langer, Y. Dong, *Nat. Rev. Mater.* **2021**, *6*, 1078.

[9] L. S. Reichel, A. Traeger, in *Handbook of Experimental Pharmacology*, (Eds: M. Schäfer-Korting, U. S. Schubert), Springer, New York **2023**, pp. 1–17.

[10] M. Neu, D. Fischer, T. Kissel, *J. Gene Med.* **2005**, *7*, 992.

[11] S. Agarwal, Y. Zhang, S. Maji, A. Greiner, *Mater. Today* **2012**, *15*, 388.

[12] J. M. Layman, S. M. Ramirez, M. D. Green, T. E. Long, *Biomacromolecules* **2009**, *10*, 1244.

[13] P. Klemm, J. I. Solomun, M. Rodewald, M. T. Kuchenbrod, V. G. Hänsch, F. Richter, J. Popp, C. Hertweck, S. Hoeppener, C. Bonduelle, S. Lecommandoux, A. Traeger, S. Schubert, *Biomacromolecules* **2022**, *23*, 4718.

[14] A. C. Rinkenauer, A. T. Press, M. Raasch, C. Pietsch, S. Schweizer, S. Schwörer, K. L. Rudolph, A. Mosig, M. Bauer, A. Traeger, U. S. Schubert, *J. Controlled Release* **2015**, *216*, 158.

[15] A. A. Eltoukhy, D. Chen, C. A. Alabi, R. Langer, D. G. Anderson, *Adv. Mater.* **2013**, *25*, 1487.

[16] E. J. Adolph, C. E. Nelson, T. A. Werfel, R. Guo, J. M. Davidson, S. A. Guelcher, C. L. Duvall, *J Mater Chem B* **2014**, *2*, 8154.

[17] A. J. Convertine, D. S. W. Benoit, C. L. Duvall, A. S. Hoffman, P. S. Stayton, *J. Controlled Release* **2009**, *133*, 221.

[18] V. Incani, A. Lavasanifar, H. Uludag, *Soft Matter* **2010**, *6*, 2124.

[19] D. H. Wakefield, J. J. Klein, J. A. Wolff, D. B. Rozema, *Bioconjugate Chem.* **2005**, *16*, 1204.

[20] X. Yue, X. Qiao, N. Qiao, S. Guo, J. Xing, L. Deng, J. Xu, A. Dong, *Biomacromolecules* **2010**, *11*, 2306.

[21] P. Van De Wetering, J.-Y. Cherng, H. Talsma, D. J. A. Crommelin, W. E. Hennink, *J. Controlled Release* **1998**, *53*, 145.

[22] J. I. Solomun, G. Cinar, P. Mapfumo, F. Richter, E. Moek, F. Hausig, L. Martin, S. Hoeppener, I. Nischang, A. Traeger, *Int. J. Pharm.* **2021**, *593*, 120080.

[23] R.-Q. Li, W. Wu, H.-Q. Song, Y. Ren, M. Yang, J. Li, F.-J. Xu, *Acta Biomater.* **2016**, *41*, 282.

[24] A. Tschiche, B. N. S. Thota, F. Neumann, A. Schäfer, N. Ma, R. Haag, *Macromol. Biosci.* **2016**, *16*, 811.

[25] F. Richter, P. Mapfumo, L. Martin, J. I. Solomun, F. Hausig, J. J. Frietsch, T. Ernst, S. Hoeppener, J. C. Brendel, A. Traeger, *J. Nanobiotechnol.* **2021**, *19*, 70.

[26] S.-Y. Lv, S. He, X.-L. Ling, Y.-Q. Wang, C. Huang, J.-R. Long, J.-Q. Wang, Y. Qin, H. Wei, C.-Y. Yu, *Int. J. Pharm.* **2022**, *627*, 122201.

[27] R. Ramachanderan, B. Schaefer, *ChemTexts* **2019**, *5*, 18.

[28] G. Gasparini, G. Sargsyan, E.-K. Bang, N. Sakai, S. Matile, *Angew. Chem.* **2015**, *127*, 7436.

[29] Q. Laurent, R. Martinent, B. Lim, A.-T. Pham, T. Kato, J. López-Andarias, N. Sakai, S. Matile, *JACS Au* **2021**, *1*, 710.

[30] M. Zheng, Y. Zhong, F. Meng, R. Peng, Z. Zhong, *Mol. Pharmaceutics* **2011**, *8*, 2434.

[31] S. Perrier, *Macromolecules* **2017**, *50*, 7433.

[32] N. Deka, A. Bera, D. Roy, P. De, *ACS Omega* **2022**, *7*, 36929.

[33] N. Deka, A. Bera, D. Roy, P. De, *Polymer* **2023**, *282*, 126158.

[34] K. Matyjaszewski, J. Xia, *Chem. Rev.* **2001**, *101*, 2921.

[35] J. I. Solomun, L. Martin, P. Mapfumo, E. Moek, E. Amro, F. Becker, S. Tuempel, S. Hoeppener, K. L. Rudolph, A. Traeger, *J. Nanobiotechnol.* **2022**, *20*, 336.

[36] C. A. Alabi, K. T. Love, G. Sahay, H. Yin, K. M. Luly, R. Langer, D. G. Anderson, *Proc. Natl. Acad. Sci. U. S. A.* **2013**, *110*, 12881.

[37] P. Patel, N. M. Ibrahim, K. Cheng, *Trends Pharmacol. Sci.* **2021**, *42*, 448.

[38] F. Hausig-Punke, F. Richter, M. Hoernke, J. C. Brendel, A. Traeger, *Macromol. Biosci.* **2022**, *22*, 2200167.

[39] R. A. Jones, M. H. Poniris, M. R. Wilson, *J. Controlled Release* **2004**, *96*, 379.

[40] O. Boussif, F. Lezoualc'h, M. A. Zanta, M. D. Mergny, D. Scherman, B. Demeneix, J. P. Behr, *Proc. Natl. Acad. Sci. U. S. A.* **1995**, *92*, 7297.

[41] A. Rémy-Kristensen, J.-P. Clamme, C. Vuilleumier, J.-G. Kuhry, Y. Mély, *Biochim Biophys Acta Biomembr* **2001**, *1514*, 21.

[42] J. Rejman, V. Oberle, I. S. Zuhorn, D. Hoekstra, *Biochem. J.* **2004**, *377*, 159.

[43] A. Fus-Kujawa, P. Prus, K. Bajdak-Rusinek, P. Teper, K. Gawron, A. Kowalczuk, A. L. Sieron, *Front. Bioeng. Biotechnol.* **2021**, *9*, 701031.

[44] S. K. Filippov, R. Khusnutdinov, A. Murmiliuk, W. Inam, L. Y. Zakharova, H. Zhang, V. V. Khutoryanskiy, *Mater. Horiz.* **2023**, *10*, 5354.

[45] W. Anderson, D. Kozak, V. A. Coleman, Å. K. Jämting, M. Trau, *J. Colloid Interface Sci.* **2013**, *405*, 322.

[46] I. Standard, Tests for in vitro cytotoxicity. Geneva, Switzerland: International Organization for Standardization **2009**, 194.

[47] T. L. Riss, R. A. Moravec, A. L. Niles, *in Mammalian Cell Viability: Methods and Protocols*, (Ed: M. J. Stoddart), Springer, New York **2011**, *740*, 103.

[48] A. Goraca, H. Huk-Kolega, A. Piechota, P. Kleniewska, E. Ciejka, B. Skibska, *Pharmacol Rep* **2011**, *63*, 849.